Engineering in Life Sciences

Eng. Life Sci. **2014**, *14*, 311–317 www.els-journal.com

Ina Dittler[1]
Stephan C. Kaiser[1]
Katharina Blaschczok[1]
Christian Löffelholz[1]
Pascal Bösch[2]
Wolfgang Dornfeld[2]
Reto Schöb[2]
Jürgen Rojahn[3]
Matthias Kraume[4]
Dieter Eibl[1]

[1]School of Life Sciences and Facility Management, Institute of Biotechnology, Zurich University of Applied Sciences, Wädenswil, Switzerland

[2]Levitronix® GmbH, Zurich, Switzerland

[3]SOPAT GmbH, Berlin, Germany

[4]Chair of Chemical and Process Engineering, Technische Universität Berlin, Berlin, Germany

Technical Report

A cost-effective and reliable method to predict mechanical stress in single-use and standard pumps

The suitability of oil–water emulsions to predict shear forces in stirred bioreactors under cost-effective and time-saving conditions has been demonstrated several times, but no application to pumps has been described so far. In this report, the drop sizes in a model oil–water system were determined for the Levitronix PuraLev® multi-use (MU) series (PuraLev® 200MU and PuraLev® 600MU), a peristaltic pump (Masterflex® I/P Easy Load), and 4-piston diaphragm pump (Quattroflow 1200-SU, where SU is single-use) using inline endoscopy. It was determined that the Sauter mean diameter could be used as a comparison criterion to estimate mechanical stress in pumps. The investigation showed that PuraLev® MU pumps are characterized by up to 59% larger Sauter mean diameters than their counterparts at comparable operational conditions. This indicates lower hydrodynamic stress in the PuraLev® MU pumps. Using computational fluid dynamics, a well-streamlined fluid flow and low turbulent energy dissipation rates were found in the PuraLev® MU pumps, which correlated well with experimental results. A calculation model was used to predict the Sauter mean diameter by combining both experimental and computational fluid dynamics data. Good agreement with deviations below 13% was determined between model predictions and experimental data.

Keywords: Emulsion / Inline endoscopy / Mechanical stress / Particle size measurement / Single-use pumps

Received: July 31, 2013; *revised:* February 18, 2014; *accepted:* March 10, 2014

DOI: 10.1002/elsc.201300068

1 Introduction

Mechanical stress can result in undesired cell damage, which is accompanied by qualitative and/or quantitative product loss [1]. In order to maintain the quality of biomass, the levels of mechanical stress need to be determined. To date, numerous studies relating to the evaluation of hydrodynamic stress on cell cultures generated by impellers in stirred tank reactors have been carried out in the biotechnological industry (e.g. [2–4]). Since pumps are also used in cell culture processes, shear forces inside the pump head also have to be considered. Previous studies have revealed that pumping processes induce mechanical stress within systems [5–7]. The magnitude of the mechanical stress depends on the type of pump and pump settings. For single-use (SU) technology based applications, which have increased in popularity during the past 10 years [8], peristaltic pumps, syringe pumps, and diaphragm pumps are commonly used. However, these pumps generate high local mechanical stresses due to the pulsating flow and pressure as well as the compression of the pump tubing. Alternative pump types reducing mechanical stress are required.

The magnetically levitated Levitronix® pump systems facilitate pulsation-free transfer of fluids. They are centrifugal pumps and have the advantage of being bearingless. In addition, use of these pumps reduces mechanical stress in fluids, as shown in hemolysis studies where thrombus formation was minimized [9–12]. Furthermore, cell death rates determined by Blaschczok et al. [13] revealed that magnetically levitated PuraLev® pumps caused lower mechanical stress to mammalian cells (Chinese hamster ovary (CHO) suspension cell line) than peristaltic and diaphragm counterparts (Masterflex® I/P Easy Load and Quattroflow 1200-SU). In addition to biological systems, non-biological model systems enable an estimation of mechanical stress under reproducible, cost-effective and time-saving

Correspondence: Ina Dittler (ina.dittler@zhaw.ch) School of Life Sciences and Facility Management, Institute of Biotechnology, Zurich University of Applied Sciences (ZHAW), Grüental, P.O. Box, 8820 Wädenswil, Switzerland

Abbreviations: CFD, computational fluid dynamics; **CHO**, Chinese hamster ovary; **MU**, multi-use; **SU**, single-use; **TEDR**, turbulent energy dissipation rates

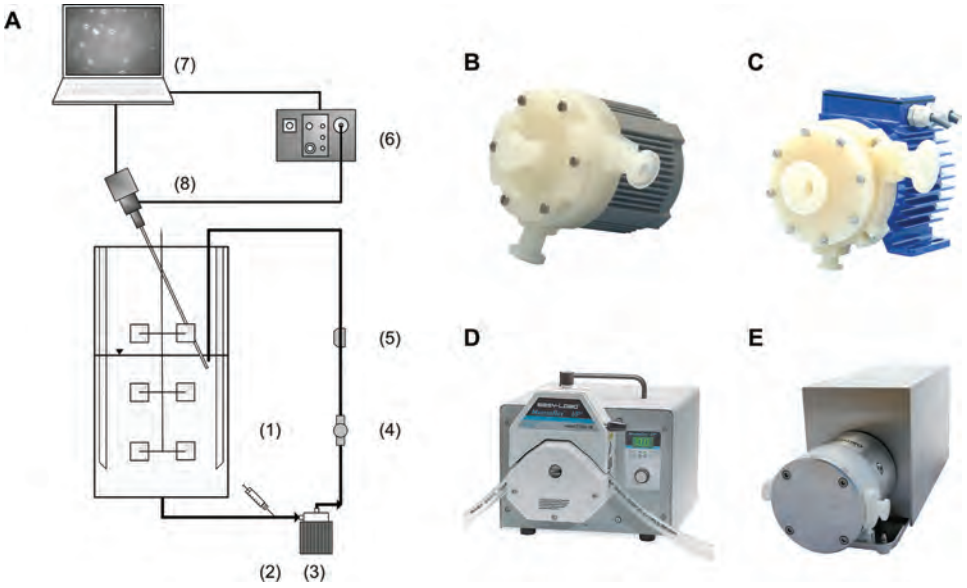

Figure 1. Setup of pump circuit are exemplarily shown for the PuraLev® 200MU and images of the pumps: (A) experimental setup, (B) PuraLev® 200MU, (C) PuraLev® 600MU, (D) peristaltic, and (E) 4–piston diaphragm pump.

conditions [14]. The use of both floccular [14–18] and oil–water emulsion systems [1, 17, 19] has already been described elsewhere. In contrast to floccular systems, oil–water emulsion systems guarantee easy detection by the use of inline endoscopy. Furthermore, the morphology of emulsion drops is comparable to mammalian cells [13]. The suitability of oil–water emulsions to predict shear forces in stirred bioreactors has been demonstrated several times (e.g. [1, 14, 20–22]), but no application to pumps has been described so far.

This paper describes the determination of Sauter mean diameters of an oil–water emulsion system in a pumping process by using inline endoscopy in combination with an automatic image analysis (SOPAT GmbH, Germany). The centrifugal-type PuraLev® multi-use (MU) pump series (Levitronix® GmbH, Switzerland), a peristaltic pump, and SU 4-piston diaphragm pump were investigated. Up to now no comparable studies have been published, so this paper is the first description of using the Sauter mean diameter as a comparison criterion to estimate the mechanical stress of conventional and SU pumps. Furthermore, experimental and computational fluid dynamics (CFD) data on PuraLev® pumps were combined to predict Sauter mean diameters, using a previously described calculation model.

2 Material and methods

2.1 Model system

All experiments were performed using a commercial oil–water emulsion, as described by Wollny [1]. First, 5 L deionized water was poured into a stirred tank and mixed with a surfactant (Triton X-100; $c_{surfactant} = 0.18$ mL/L). After complete dissolution of the surfactant, oil (Mobil EAL Arctic 22, Eberhart Schmierstoffe AG, Germany; $c_{oil} = 1.28$ mL/L) was added via the syringe port and distributed by the investigated pump (PuraLev® 200MU, PuraLev® 600MU, Quattroflow 1200-SU, Masterflex® I/P Easy Load; Fig. 1A and B).

2.2 Experimental setup and pump types

The cylindrical, baffled stirred tank (Fig. 1A) was equipped with three Rushton turbines, which were exclusively used to mix the surfactant. During the pumping process, the impellers were not used. The fluid was circulated by the pump in a closed loop. As shown in Fig. 1A, the oil was added via a syringe port (2) in front of the pump (3) and was homogeneously distributed throughout the reactor by the pumping process (1). A clamp-on flow meter (4) (Levitronix® GmbH, Switzerland) and a SU pressure sensor (5) (SciLog BioProcessing Systems, USA) were integrated into the closed loop to monitor the volume flow rate and pressure for different pump settings. The endoscope probe (8) (SOPAT-VF; SOPAT GmbH, Germany) was equipped with a charge-coupled device camera to record images of the emulsion drops inside the vessel. In order to guarantee sharp pictures, a strobe flash was triggered and then reflected in a rhodium mirror at the tip of the endoscope lens through a fiber optic cable (6). Subsequently, the images were processed using automated analysis software on a separate computer (7). The experiments were carried out for two different sizes of centrifugal PuraLev® MU pumps (PuraLev® 200MU and PuraLev® 600MU, Levitronix® GmbH, Switzerland; Fig. 1B and C), which were compared to a peristaltic pump (Masterflex® I/P Easy Load, Cole Parmer, USA) and a 4-piston diaphragm pump (Quattroflow 1200-SU, Almatechnik AG, Switzerland; Fig. 1D and E). The investigations were performed at a constant flow rate of 3.4 L/min and with identical pressure drops in the range of 0.03–0.61 bar, which were varied by using a hose clamp and by selecting different tubing lengths and diameters. It was found that the pressure loss in front of the pump was negligible, so that pressure measurement was only required behind the pump.

2.3 Measurement and image analysis

For all experiments, a 16-mm-thick inline endoscope probe (SOPAT-VF; Fig. 1A) was introduced into the tank directly

beneath the inlet in order to guarantee that individual drops were not recorded more than once, even at low rates. To generate real-time images, the probe-based microscope was connected to a high-speed camera and stroboscope. Simultaneously, the camera and strobe flash were triggered by the image acquisition SOPAT-CamControl to ensure high-contrast images. As the probe is capable of measuring drops from 5 to 350 μm, the technique was suitable for determining drop sizes in a pumping process. Over the experiment time of 1 h, 50 images were recorded every minute with a frame rate of 7.5 frames per second. In doing so, at least 300 drops were detected at each measurement point, guaranteeing statistical certainty [22]. Automatic image recognition provided by the SOPAT software (SOPAT GmbH, Germany, www.sopat.de) was realized to determine the drop size distribution. Panckow et al. [23] provide an overview of the measurement principle and describe the particle recognition process. The drop sizes are expressed by the Sauter mean diameter, which is most commonly used as the representative diameter of particles in dispersions. The Sauter mean diameter is defined as

$$d_{32} = \frac{\Sigma d_p^3}{\Sigma d_p^2}. \quad (1)$$

2.4 Numerical model

The fluid flow patterns of the PuraLev® 200MU and PuraLev® 600MU pumps were simulated by means of a CFD code (Fluent 14.0 by ANSYS, Inc.). This approach was already described in detail by Blaschczok et al. [13]. Briefly, the fluid domains of the centrifugal pumps were subdivided into two zones to describe impeller rotation using the multiple reference frames methodology, with the inner zone containing the rotor. Body-fitted unstructured grids consisting of approximately $2.5 \cdot 10^6$ (PuraLev® 200MU) and $3.7 \cdot 10^6$ (PuraLev® 600MU) control volumes were generated to spatially discretize the fluid domains. Assuming a time-invariant fluid flow, the Reynolds averaged mass and momentum equations were solved using the standard k-ε turbulence model as provided by Fluent. The walls of the pump housing and impeller were treated as nonslip boundaries with standard wall functions. The flow rates and pressure drops were defined by inlet velocity and pressure outlet conditions, respectively. All equations were discretized using the first-order upwind scheme, and semi-implicit method for pressure-linked equations (SIMPLE) algorithm was chosen for pressure–velocity coupling. Convergence was assumed when the residuals decreased to below 10^{-5}. To date, simulations are not available for the 4-piston diaphragm and peristaltic pumps, because their fluid domains change over time.

3 Results and discussion

3.1 Drop size as a measure of hydrodynamic stress

3.1.1 Sauter mean diameter

For all experiments, the Sauter mean diameter decreased over the pumping time and reached a steady state at the end of the experiment. By way of example, the curve shapes for the centrifugal PuraLev® 200MU pump and the peristaltic pump were compared with each other (Fig. 2A and B). As shown in Fig. 2A, the Sauter mean diameter decreased from $d_{32,0\,min} = 78$ μm to $d_{32,60\,min} = 33$ μm during the experiment for the PuraLev® 200MU at a pressure drop of 0.03 bar. Furthermore, smaller drop sizes were determined as the pressure drop increased. This indicated that mechanical stress was dependent on impeller speed in the PuraLev® 200MU (Fig. 2A), which is in agreement with previous findings with CHO suspension cells [13]. The Sauter mean diameter for the peristaltic pump was $d_{32,60\,min} = 10$ μm at the end of the pumping process for all pressure settings (Fig. 2B). These results show that the Sauter mean diameters are independent of the pressure drop and dependent on the mechanical stress in the pumps used; the higher the mechanical stress, the smaller the Sauter mean diameter.

In spite of single measurements, at least 300 drops were detected at each measurement point, so that statistical certainty is guaranteed. The highest deviations were calculated for the PuraLev® 200MU ($d_{32,4\,min} \pm 42$ μm) and PuraLev® 600MU ($d_{32,6\,min} \pm 21$ μm) at a pressure drop of 0.03 bar in the first few minutes. The Sauter mean diameter decreased with increasing pumping time and pressure drop ending in standard deviations (SDs) no greater than $d_{32} \pm 0.5$ μm for both the PuraLev® 200MU and PuraLev® 600MU in the remaining time. In contrast to the centrifugal pump types, the comparison pumps showed SDs below $d_{32} \pm 1.9$ μm at a pressure drop ranging from 0.03 to 0.61 bar.

3.1.2 Drop size distribution

It is well known that the Sauter mean diameter can be significantly influenced by single drop sizes, and especially by larger drops, because of the cube of the drop diameter in Eq. (1). Therefore, drop sizes are given in a semilogarithmical, cumulative number distribution Q_0 (class number: 50) at the beginning ($t_{0\,min}$) and at the end ($t_{60\,min}$) of the experiment for the PuraLev® 200MU and peristaltic pump, at a flow rate of 3.4 L/min and a pressure drop of 0.61 bar (Fig. 2C). This enables a comparison of drop size between two different time points. It can be seen that similar drop size distributions were detected in a range from 10 to 100 μm. The drop size distributions can be approximated by log-normal functions, since a larger number of small drops were detected in the peristaltic pump and the curve is steeper than for the centrifugal-type PuraLev® 200MU for both time points ($t_{0\,min}$; $t_{60\,min}$). As pumping time increased, the drop sizes in both the PuraLev® 200MU and the peristaltic pump decreased. It should be emphasized that the drop size class with the largest volume fraction was close to the lower detection limit of the photo-optical measurement technique used.

3.1.3 Measured Sauter mean diameter as comparison criterion

After 50 min, the Sauter mean diameter reached a steady state and thus the average value of the Sauter mean diameters measured in the last 10 min was used as a comparison criterion (measured Sauter mean diameter $d_{32,m}$) to estimate the mechanical stress of the investigated PuraLev® MU pumps, the peristaltic pump and 4-piston diaphragm pump. The measured Sauter mean diameters $d_{32,m}$ for all investigations are shown in Fig. 2D. The largest drops of $d_{32,m} = 36$ μm were obtained at

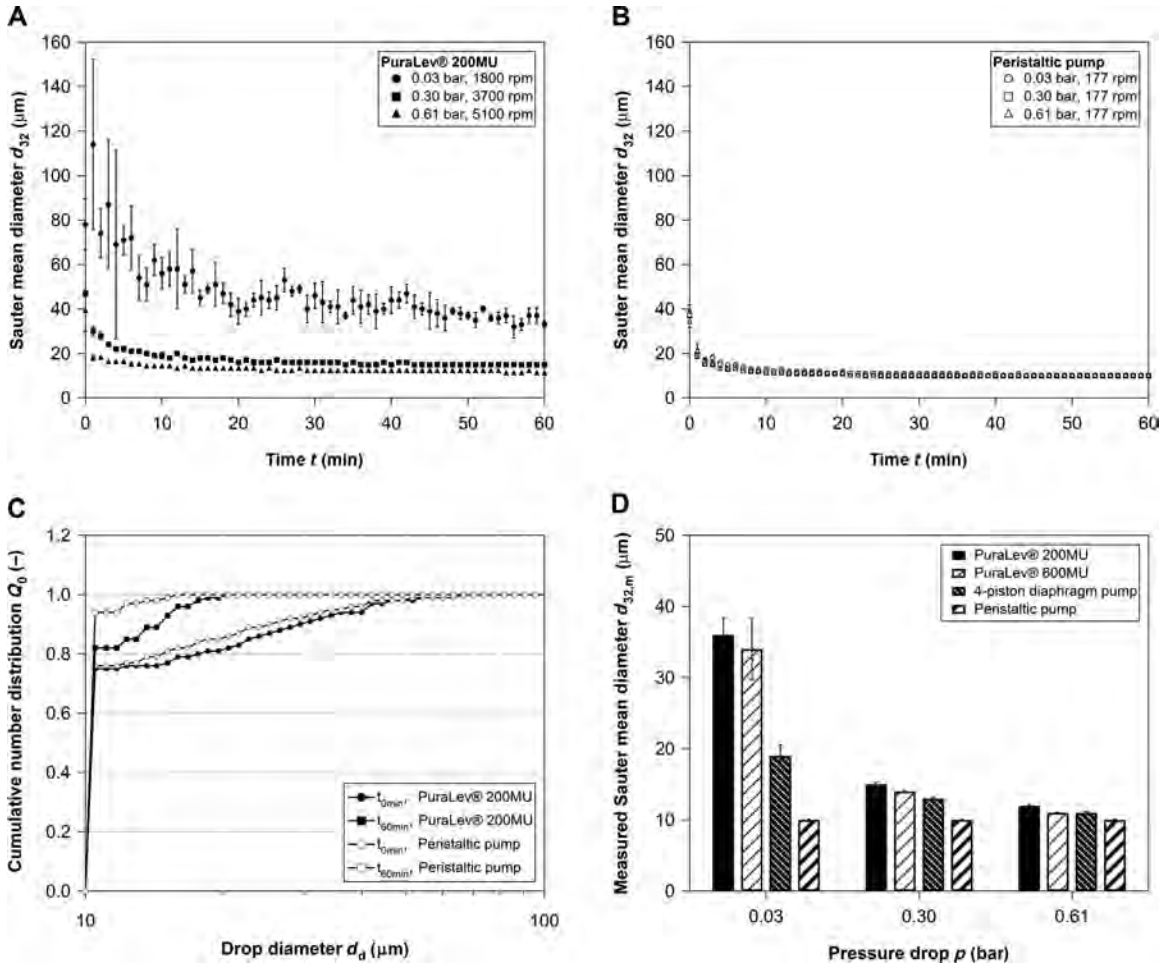

Figure 2. Comparison of the Sauter mean diameter: (A) Sauter mean diameters d_{32} for the PuraLev® 200MU and (B) for the peristaltic pump, (C) cumulative number distribution Q_0 for the PuraLev® 200MU and the peristaltic pump, (D) measured Sauter mean diameter $d_{32,m}$ for the PuraLev® 200MU, PuraLev® 600MU, 4-piston diaphragm pump, and the peristaltic pump. The Sauter mean diameters d_{32} and the measured Sauter mean diameters $d_{32,m}$ were determined at a flow rate of 3.4 L/min and a pressure drop ranging from 0.03 to 0.61 bar. The cumulative number distributions Q_0 are exemplarily shown at the beginning ($t_{0\,min}$) and the end ($t_{60\,min}$) of the experiment for a flow rate of 3.4 L/min and a pressure drop of 0.61 bar. The resulting SD of the different Sauter mean diameters d_{32} ($n \geq 300$) and measured Sauter mean diameters $d_{32,m}$ ($n = 10$) are shown.

0.03 bar with the PuraLev® 200MU. Under the same conditions, the PuraLev® 600MU showed a similar drop size ($d_{32,m} = 34\ \mu m$). In contrast to the PuraLev® MU series, the comparison pumps exhibited a smaller measured Sauter mean diameter $d_{32,m}$ of 19 μm for the 4-piston diaphragm and 10 μm for the peristaltic pump, indicating stronger mechanical stress in the emulsion system. In general, a decrease in the measured Sauter mean diameters was observed for the PuraLev® 200MU, the PuraLev® 600MU and the 4-piston diaphragm pump with increasing mechanical stress. In contrast, the peristaltic pump showed a measured Sauter mean diameter of $d_{32,m} = 10\ \mu m$ for all pressure settings, thus, the mechanical stress was independent of the pressure drop for the peristaltic pump, which is in agreement with previous findings with CHO suspension cells [13].

Moreover, it should be noted that the variation between the average values of Sauter mean diameters in the last 10 min and the SDs became smaller as the pressure drop increased. The highest SDs were calculated for the PuraLev® 200MU ($d_{32,m} \pm 2.4\ \mu m$) and PuraLev® 600MU ($d_{32,m} \pm 4.3\ \mu m$) at a pressure drop of 0.03 bar.

3.2 Fluid flow pattern

The predicted fluid flow pattern in the PuraLev® 200MU and PuraLev® 600MU was found to agree well with previous investigations, which are explained in detail by Blaschczok et al. [13]. Briefly, the fluid enters the PuraLev® pump through the inlet, is subsequently redirected by 90°, and transported outwards through the blade-to-blade passage. In the blade-to-blade passage, the fluid quickly gains momentum and enters the volute. As is typical of centrifugal-type pumps, it was found that the flows in the four blade channels were similar to each other. This was also described by Chua et al. [24] for a

centrifugal-type blood pump. The authors stated that the axially symmetric design allowed the magnetically suspended impeller to be easily controlled for more balanced radial thrusting force. Similar to the findings of Zhang et al. [12], no visible small localized vortexes or flow disturbances were observed in the region between the blades. Furthermore, the flow in the PuraLev® 200MU was predominantly tangential with only low axial dispersion through the gap between the impeller and housing. In contrast to the PuraLev® 200MU, the PuraLev® 600MU displayed a secondary flow through the rotor central core, which was similar to the flow described by Zhang et al. [12] for the CentriMag® and by Taskin et al. [25] for the Levitronix UltraMag® blood pump. In the PuraLev® 600MU, a portion of the fluid flowed axially downwards through the gap between the impeller and housing cavity walls, and provided an excellent surface washing in the gap. In general, the fluid flow pattern was well streamlined and aligned for both the PuraLev® 200MU and PuraLev® 600MU, which corresponded with the findings of Zhang et al. [12].

Based on steady-state fluid flow, the local dissipation rates were estimated in order to predict drop size for the PuraLev® MU pumps. The representative turbulent energy dissipation rates (TEDR) for both the PuraLev® 200MU and PuraLev® 600MU were determined at each pump setting from the CFD predictions based on the volume-weighted frequency distribution of the TEDR. These distributions were qualitatively and quantitatively comparable to data obtained in previous studies with the PuraLev® 200MU published by Blaschczok et al. [13]. The CFD results showed small TEDR in a large amount of the control volume (≈ 95%), which dominated the drop breakup. Thus, the representative TEDR were determined at a maximal volume fraction of the fluid domain. With increasing impeller speed (i.e. pressure difference), the representative TEDR increased from 3.4 to 91.5 m^2/s^3 in the PuraLev® 200MU and from 4.1 to 72.2 m^2/s^3 in the PuraLev® 600MU. In comparison to investigations on the hydrodynamic sensitivity of mammalian cells, the TEDR determined were lower by two orders of magnitude than the threshold energy dissipation rate for lethal cell damage of $6.4 \cdot 10^3$ m^2/s^3 reported by Godoy-Silva [3]. The highest TEDR were found in small volume fractions of the fluid domain, for example the gap between the impeller and housing, and at the surface of the impeller near the impeller tips, which was negligible for these investigations.

3.3 Calculation of the predicted Sauter mean diameter

An initial calculation model was carried out by Shinnar [21] using the impeller's Weber number. On this basis, further work was performed by Lee et al. [26], Zerfa and Brooks [27], and Angle and Hamza [28], which considered the breakup of drops in a coalescing system (Eq. 2). The value of the constant C depends on the impeller type and C_1 reflecting the tendency of drops to coalesce. It was therefore decided to test the equations developed in the above-mentioned studies for their applicability to this investigation.

$$\frac{d_{32}}{d} = \mathrm{C} \cdot (1 + C_1 \cdot \phi)\, \mathrm{We}^{-0.6} \tag{2}$$

The application of Eq. (2) showed a deviation of over 76% as a result of the predicted Sauter mean diameter calculation being affected by empiric, process-related constants. In contrast, the universal approach by Wollny [1] shows more promising results. Equation (3) presents the correlation between power consumption as well as impeller speed, and can be used to determine drop size in inertial ($b = 2/5$) and viscous ranges ($b = 1/3$). In general, Wollny's [1] approach includes three different correlation equations. These equations (Eq. 3) represent three different ways of calculating the predicted Sauter mean diameter. For example, Eq. (4) describes the relationship between the power input and predicted Sauter mean diameter $d_{32,\mathrm{p}}$.

$$d_{32,\mathrm{p}} = C_2 \cdot \varepsilon^{-\mathrm{b}} = C_3 \cdot u^{-3\mathrm{b}} = C_4 \cdot \mathrm{We}^{-1.5\mathrm{b}} \tag{3}$$

$$d_{32,\mathrm{p}} = C_2 \cdot \varepsilon^{-\mathrm{b}} \tag{4}$$

The power input constant C_2 is a function of the number of tests N, the measured Sauter mean diameter $d_{32,\mathrm{m}}$, and the representative TEDR ε (Eq. 5).

$$C_2 = \frac{1}{N} \sum_{i=1}^{N} \left(d_{32,\mathrm{m}} \cdot \varepsilon^{\mathrm{b}} \right) \tag{5}$$

The applied constants are interdependent; thus, the rotation speed constant C_3 can be calculated from C_2 (Eq. 6) and the constant for the Weber number C_4 from C_3 (Eq. 7).

$$\mathrm{C}_3 = \mathrm{C}_2 \cdot \varepsilon^{-b} \cdot u^{3b} \tag{6}$$

The equation for the constant C_4 includes the Weber number ($\mathrm{We} = \rho_c \cdot n^2 \cdot d_1^3 \cdot \gamma^{-1}$) and peripheral speed ($u = \pi \cdot d_1 \cdot n$), where n is the impeller speed, d_1 is the diameter of the pump impeller, and γ is the interfacial tension.

$$\mathrm{C}_4 = \mathrm{C}_3 \cdot \left(\frac{\rho_c \cdot d_1}{\gamma \cdot \pi^2} \right)^{1.5b} \tag{7}$$

In this case, the predicted Sauter mean diameters were determined in viscous range. As shown in Table 1, good agreement between the predicted and measured Sauter mean diameters ($d_{32,\mathrm{p}}$, $d_{32,\mathrm{m}}$) was obtained for all pump settings for the PuraLev® MU pumps. Smaller drop sizes were generated by the PuraLev® 600MU, indicating higher mechanical stresses compared to the PuraLev® 200MU. This result is in line with the experimental measurement. Finally, the calculation of the predicted Sauter mean diameter $d_{32,\mathrm{p}}$ resulted in a deviation lower than 13% when using the correlation with Eq. (3). Thus, the calculation models can be used to determine the predicted Sauter mean diameter in accordance with Wollny's model [1].

4 Concluding remarks

The estimation of mechanical stress during pumping processes is beneficial as it contributes to the reduction of cell damage to shear sensitive cells used in biopharmaceutical manufacturing. In contrast to biological systems, model emulsion systems enable mechanical stress to be predicted under time-saving, cost-effective, and reproducible conditions [1]. To estimate mechanical stress in pumps, emulsion drops were detected using inline endoscopy, whose suitability for reliable drop size detection in

Table 1. A comparison of the measured Sauter mean diameter with predictions as a function of power input (Eq. 4) based on the Wollny's model [1]

Pump	p (bar)	n (rpm)	ε (m^2/s^3)	d_{32} (μm)		Relative deviation (%)
			CFD predicted	Predicted $d_{32,p}$	Measured $d_{32,m}$	
PuraLev® 200MU	0.03	1800	3	35	36	3.9
	0.30	3700	31	16	15	9.3
	0.61	5100	91	12	12	4.3
PuraLev® 600MU	0.03	1600	4	30	34	12.1
	0.30	3100	29	16	14	10.9
	0.61	4200	72	11	11	4.1

liquid/liquid model systems is known [1, 29–32]. However, the application of this particular measurement technique to pumping systems was successfully demonstrated for the first time. The inline endoscope technique showed low SDs (below 15%) in the measured Sauter mean diameter, which indicates reliability of drop size measurement. Wollny [1] already showed the dependency of drop sizes on mechanical stress, which was confirmed by this study. Consequently, the investigations revealed that the Sauter mean diameter is suitable for the comparison of different pumps (PuraLev® 200MU, PuraLev® 600MU, 4-piston diaphragm and peristaltic pump) under similar conditions (i.e. pressure drop and flow rate). In contrast to the bearingless PuraLev® MU pumps, the comparison pumps were found to have smaller measured Sauter mean diameters, indicating higher hydrodynamic stress and agreeing with previous investigations using CHO suspension cells [13]. So far, the PuraLev® 200MU generated the lowest mechanical stress and the peristaltic pump generated the highest mechanical stress under the tested operational conditions. The CFD simulations showed a well-streamlined and aligned fluid flow as well as representative TEDR, which were two orders of magnitude lower than those that cause cell lysis [3]. Furthermore, the representative TEDR obtained for the centrifugal pump were used to determine the predicted Sauter mean diameters based on a model originally developed for stirred vessels [1]. Good agreement with deviations below 13% was found between the predicted and measured Sauter mean diameters. Thus, the model can be applied to the pumps investigated, although a wider range of operational conditions need to be considered as part of future studies.

Practical application

The development of shear sensitive pumps is necessary to avoid cell or even product damage in the biotechnological industry. As a result, conventional and SU pumps intended for use under aseptic conditions have to be designed in such a way that they generate low levels of mechanical stress. In this study, Sauter mean diameters were determined by a cost-effective and time-saving method that used a model oil–water emulsion system. This is the first description of using the steady-state Sauter mean diameter as a comparison criterion to estimate the mechanical stress inside different pumps.

The authors would like to thank the Commission for Technology and Innovation (CTI, Switzerland) for their financial support (no. 13236.1 PFFLI-LS).

The authors have declared no conflict of interest.

Nomenclature

$\dot{V}$	[m^3/s]	Flow rate
C	[-]	Constant
c	[m^3/m^3]	Concentration
d	[m]	Stirrer diameter
d_{32}	[m]	Sauter mean diameter
$d_{32,m}$	[m]	Measured Sauter mean diameter
$d_{32,p}$	[m]	Predicted Sauter mean diameter
d_d	[m]	Drop diameter
d_I	[m]	Pump impeller diameter
k	[m^2/s^2]	Turbulent kinetic energy
N	[-]	Number of tests
n	[s^{-1}]	Impeller speed
p	[Pa]	Pressure drop
Q_0	[-]	Cumulative number distribution
t	[s]	Time
u	[m/s]	Peripheral speed
We	[-]	Weber number
Greek symbols		
γ	[N/m]	Interfacial tension
ε	[m^2/s^3]	(Turbulent) energy dissipation rate
ρ_c	[kg/m^3]	Fluid density of the continuous phase
ϕ	[-]	Volume fraction of dispersed phase

5 References

[1] Wollny, S., Experimentelle und numerische Untersuchungen zur Partikelbeanspruchung in gerührten (Bio-) Reaktoren. PhD thesis, Technische Universität Berlin, Berlin 2010.

[2] Leupold, M., Hindersin, S., Gust, G., Kerner, M. et al., Influence of mixing and shear stress on *Chlorella vulgaris*, *Scenedesmus obliquus*, and *Chlamydomonas reinhardtii*. *J. Appl. Phycol.* 2013, *25*, 485–495.

[3] Godoy-Silva, R., Chalmers, J., Casnocha, S., Bass, L. et al., Physiological responses of CHO cells to repetitive hydrodynamic stress. *Biotechnol. Bioeng.* 2009, *103*, 1103–1117.

[4] Siecka, J. B., Cordes, T., Budach, W., Rhiel, M. H. et al., Development of a scale-down model of hydrodynamic stress to study the performance of an industrial CHO cell line under simulated production scale bioreactor conditions. *J. Biotechnol.* 2013, *164*, 41–49.
[5] Jaouen, P., Vandanjon, L., Quéméneur, F., The shear stress of microalgal cell suspension (*Tetraselmis suecica*) in tangential flow filtration systems: The role of pumps. *Bioresour. Technol.* 1999, *68*, 149–154.
[6] Bee, J. S., Stevenson, J. L., Mehta, B., Svitel, J. et al., Response of a concentrated monoclonal antibody formulation to high shear. *Biotechnol. Bioeng.* 2009, *103*, 936–943.
[7] Klaus, S., Bluttraumatisierung bei der Passage zeitkonstanter und zeitvarianter Scherfelder. PhD thesis, RWTH Aachen University, Aachen 2004.
[8] Eibl, R., Eibl, D., Disposable bioreactors for cell culture-based bioprocessing. *ACHEMA Worldwide News* 2007, *2*, 8–10.
[9] Aggarwal, A., Modi, S., Kumar, S., Kooapati, C. et al., Use of a single-circuit CentriMag® for biventricular support in postpartum cardiomyopathy. *Perfusion* 2012, *28*, 156–159.
[10] Kouretas, P. C., Kaza, A. K., Burch, P. T., Witte, M. K. et al., Experience with the Levitronix CentriMag® in the pediatric population as a bridge to decision and recovery. *Artif. Organs* 2009, *33*, 1002–1004.
[11] Khan, N. U., Al-Aloul, M., Shah, R., Yonan, N., Early experience with the Levitronix CentriMag® device for extra-corporeal membrane oxygenation following lung transplantation. *Eur. J. Cardiothorac. Surg.* 2008, *34*, 1262–1264.
[12] Zhang, J., Gellman, B., Koert, A., Dasse, K. A. et al., Computational and experimental evaluation of the fluid dynamics and hemocompatibility of the CentriMag blood pump. *Artif. Organs* 2006, *30*, 168–177.
[13] Blaschczok, K., Kaiser, S. C., Löffelholz, C., Imseng, N. et al., Investigations on mechanical stress caused to CHO suspension cells by standard and single-use pumps. *Chem. Ing. Tech.* 2012, *85*, 144–152.
[14] Henzler, H.-J., Particle stress in bioreactors. *Adv. Biochem. Eng. Biotechnol.* 2000, *67*, 35–82.
[15] Biedermann, A., Henzler, H.-J., Beanspruchung von Partikeln in Rührreaktoren. *Chem. Ing. Tech.* 1994, *66*, 209–211.
[16] Hoffmann, J., Büscher, K., Hempel, D. C., Ermittlung von maximalen Scherspannungen in Rührbehältern. *Chem. Ing. Tech.* 1995, *76*, 210–214.
[17] Henzler, H.-J., Biedermann, A., Modelluntersuchungen zur Partikelbeanspruchung in Reaktoren. *Chem. Ing. Tech.* 1996, *68*, 1546–1561.
[18] Pohlscheidt, M., Entwicklung und Optimierung eines Verfahrens zur Viruspropagation von *Parapoxvirus Ovis NZ-2*. PhD thesis, Otto von Guericke University Magdeburg, Magdeburg 2005.
[19] Wollny, S., Sperling, R., Kraume, M., Beanspruchung von Partikeln und Fluidelementen beim Rühren. *Chem. Ing. Tech.* 2007, *79*, 1024–1028.
[20] Sprow, F. B., Drop size distributions in strongly coalescing agitated liquid-liquid systems. *AIChE J.* 1967, *13*, 995–998.
[21] Shinnar, R., On the behaviour of liquid dispersions in mixing vessels. *J. Fluid Mech.* 1961, *10*, 259–275.
[22] Ritter, J., Kraume, M., Online measurement technique for drop size distributions in liquid/liquid systems at high dispersed phase fractions. *Chem. Eng. Technol.* 2000, *23*, 579–581.
[23] Panckow, R., Maaß, S., Emmerich, J., Kraume, M., Automatisierte Quantifizierung von Blasengrößenverteilungen in einem gerührten Luft/Wasser-System. *Chem. Ing. Tech.* 2013, *85*, 1036–1045.
[24] Chua, L. P., Song, G., Lim, T. M., Zhou, T., Numerical analysis of the inner flow field of a biocentrifugal blood pump. *Artif. Organs* 2006, *30*, 467–477.
[25] Taskin, M. T., Fraser, K. H., Zhang, T., Gellman, B. et al., Computational characterization of flow and hemolytic performance of the UltraMag blood pump for circulatory support. *Artif. Organs* 2010, *34*, 1099–1113.
[26] Lee, J. C., Tasakorn, P., Belghazi, A., Fundamentals of drop breakage in the formation of liquid-liquid dispersions. *Proceedings of the Third European Conference on Mixing—The Formation of Liquid-Liquid Dispersions Chemical and Engineering Aspects*, Vol. *157*, BHRA, New York 1979, pp. 43–57.
[27] Zerfa, M., Brooks, B. W., Prediction of vinyl chloride drop sizes in stabilised liquid–liquid agitated dispersion. *Chem. Eng. Sci.* 1996, *51*, 3223–3233.
[28] Angle, C. W., Hamza, H. A., Predicting the sizes of toluene-diluted heavy oil emulsions in turbulent flow. Part 2: Hinze-Kolmogorov based model adapted for increased oil fractions and energy dissipation in a stirred tank. *Chem. Eng. Sci.* 2006, *61*, 7325–7335.
[29] Maaß, S., Wollny, S., Sperling, R., Kraume, M., Numerical and experimental analysis of particle strain and breakage in turbulent dispersions. *Chem. Eng. Res. Des.* 2009, *87*, 565–572.
[30] Maaß, S., Grünig, J., Kraume, M., Measurement techniques for drop size distributions in stirred liquid-liquid systems. *Chem. Process Eng.* 2009, *30*, 635–651.
[31] Maaß, S., Wollny, S., Voigt, A., Kraume, M., Experimental comparison of measurement techniques for drop size distributions in liquid/liquid dispersions. *Exp. Fluids* 2011, *50*, 259–269.
[32] Maaß, S., Metz, F., Rehm, T., Kraume, M., Prediction of drop sizes for liquid/liquid systems in stirred slim reactors—Part I: Single stage impellers. *Chem. Eng.* 2010, *162*, 792–801.